Lactobionic acid and carboxymethyl chitosan functionalized graphene oxide nanocomposites as targeted anticancer drug delivery systems

Qixia Pan[a] *E-Mail: 18201763956@163.com*

Yao Lv[a] *E-Mail: LvYao2014year@126.com*

Gareth R. Williams[b] *E-Mail:* g.williams@ucl.ac.uk

Lei Tao[a] *E-Mail: taolei89757@163.com*

Huihui Yang[a] *E-Mail: yhhdr_2009@163.com*

Heyu Li[a] *E-Mail: heyu.li@qq.com*

Limin Zhu[a*] *E-Mail: lzhu@dhu.edu.cn*

[a] *College of Chemistry, Chemical Engineering and Biotechnology, Donghua University, Shanghai 201620, PR China*

[b] *UCL School of Pharmacy, University College London, 29-39 Brunswick Square, London, WC1N 1AX, UK*

** Corresponding author contact information. E-Mail: lzhu@dhu.edu.cn; Tel.: 021-67792655; Fax: 021-67792655*

Abstract

In this work, we report a targeted drug delivery system built by functionalizing graphene oxide (GO) with carboxymethyl chitosan (CMC), fluorescein isothiocyanate and lactobionic acid (LA). Analogous systems without LA were prepared as controls. Doxorubicin (DOX) was loaded onto the composites through adsorption. The release behavior from both the LA-functionalized and the LA-free material is markedly pH sensitive. The modified GOs had high biocompatibility with the liver cancer cell line SMMC-7721, but can induce cell death after 24 h incubation if loaded with DOX. Tests with shorter (2 h) incubation times were undertaken to investigate the selectivity of the GO composites: under these conditions, neither DOX-loaded system was found to be toxic to the non-cancerous L929 cell line, but the LA-containing composite showed the ability to selectively induce cell death in cancerous (SMMC-7721) cells while the LA-free analogue was inactive here also. These findings show that the modified GO materials are strong potential candidates for targeted anticancer drug delivery systems.

Keywords: Graphene oxide, lactobionic acid, doxorubicin, ASGPRS receptor, pH sensitive, targeted delivery,

1. Introduction

A potent drug delivery system (DDS) must both achieve targeted delivery and a controlled rate of drug release. Such a system not only improves therapeutic efficacy, but also minimizes associated side effects. A vast number of DDSs have been developed (Arora, Al, Ahuja, Khar, & Baboota, 2005; Debbage, 2009; Bruschi, 2015; Allen & Cullis, 2013; Gong, Chen, Zheng, Wang, & Wang, 2012; Bamrungsap, et al., 2012; Bae, & Park, 2011); in the last 10 years or so, carbon based nanostructures – most notably carbon nanotubes (CNTs) – have attracted particular attention in this regard (Bianco, Kostarelos, & Prato, 2005; Liu, et al., 2008; Feazell, Nakayama-Ratchford, Dai, & Lippard, 2007; Zhang, Zhang, & Zhang, 2011; Meng, Zhang, Lu, Fei, & Dyson, 2012; Zhu, et al., 2014; Faria, et al., 2014). Graphene oxide (GO) has been less explored than CNTs but offers a number of potential advantages, including an ultrahigh surface area for physical adsorption of a drug (mainly through π-π stacking) (Sun, et al., 2008; Liu, Robinson, Sun, & Dai, 2008) and abundant oxygen-containing functional groups (carboxyl groups, hydroxyl groups and epoxy groups), which make it dispersible in aqueous media and impart it with the ability to be further modified with functional molecules (Ma, et al., 2012; Bao, et al., 2011).

The first report of GO used as a DDS came from Sun et. al. in 2008 (Sun, et al, 2008). These authors synthesized nanoscale GO sheets, developed functionalization chemistry to permit GO to remain soluble in physiological media, and also proved that doxorubicin, a potent anti-cancer drug, could be adsorbed to the sheets and delivered to cells in vitro. At around the same time, Yang and co-workers independently reported the adsorption and release of doxorubicin using GO (Lv, et al., 2012). Since then, there has been an explosion of interest in using GO for drug delivery purposes. The key features of GO causing it to attract this attention are its effective transportation capability, high levels of cellular uptake, and lack of obvious toxicity (Zhang, et al., 2015). These properties have caused GO to be investigated in particular for the targeted cellular delivery of anticancer drugs (Zhang, Xia, Zhao, Liu,

& Zhang, 2010; Tao, et al., 2012; Long, et al., 2013).

In order to maximize its functionality as a biomaterial, GO is often modified in order to prevent aggregation and ensure compatibility with biological tissue. Polyethylene glycol (PEG) has been used to this end (Sun, et al., 2008; Ma, et al., 2012; Wen, et al., 2012), but another option is the naturally occurring chitosan material. This has been widely used in the biomaterial field due to its biodegradability and non-toxicity (Agnihotri, Mallikarjuna, & Aminabhavi, 2004; Jayakumar, Prabaharan, Kumar, Nair, & Tamura, 2011; Shan, et al., 2010; Roosen, Spooren, & Binnemans, 2014), but suffers from poor water solubility (Zheng, et al., 2011). To overcome this problem, chitosan can be derivatized to give carboxymethyl chitosan (CMC), a material which has shown excellent biocompatibility (Luo, Teng, & Wang, 2012; Vaghani, Patel, & Satish, 2012). CMC, which contains a number of amino groups, can be used to modify GO to improve its dispersibility in water and physiological environment through covalent functionalization (Zheng, et al., 2011). Very recently, Yang et al. have employed CMC-modified GO to prepare doxorubicin-loaded hyaluronic acid-functionalized systems for targeted delivery to cancer cells (Yang, et al., 2016). The materials produced had excellent dispersibility and biocompatibility, and displayed pH-sensitive drug release: release at the cancer microenvironment pH of 5.8 was faster and reached a higher percentage of the drug loading than at the general physiological pH of 7.4. Further, the composites were taken up effectively by cancerous HeLa cells, but not by non-cancerous L929 cells, and the latter were largely unaffected by being incubated with the GO composites while the HeLa cells were much reduced in their viability (Yang, et al., 2016).

One way to achieve targeted drug delivery to a particular cellular population is to exploit particular biological signatures of the cell type of interest. The high levels of expression of asialoglycoprotein receptors (ASGPRs) on the surface of hepatocytes (Ashwel & Harford, 1982) have been widely utilized in this regard. ASGPRs bind galactose moieties and thus lactobionic acid (LA), a disaccharide comprising gluconic acid and galactose, can be employed to develop liver-targeted DDSs. This technology can be coupled with pH-sensitive components to yield a system which can both target liver cells and also ensure that drug release only occurs in the acidic microenvironment typical of cancerous cells (Zhang, Meng, Lu, Fei, & Dyson, 2009). LA has been used to functionalize a number of different carriers such as magnetite nanoparticles (Song, et al., 2015) and laponite (a synthetic clay) (Chen, et al., 2015) for targeted drug delivery, or dendrimer-entrapped gold nanoparticles for computed tomography imaging applications (Cao, et al., 2015). However, the possibility of using functionalized GO to target hepatocytes via this route has not been explored.

In this study, a drug delivery system based on graphene oxide, carboxymethyl chitosan and lactobionic acid was developed and loaded with the anti-cancer drug doxorubicin. We hypothesized that the GO-CMC materials (both LA functionalized and LA free) could be effectively loaded with DOX, and would give more rapid release at the lower pH typical of the cancer cell microenvironment than at the general physiological pH. We further anticipated that functionalization of the GO-CMC composites with LA would permit their selective uptake by cancerous cells with only minimal uptake by non-cancerous cells, and thus that the LA-containing materials would be able to act as precisely targeted anti-cancer drug delivery systems.

2. Experimental

2.1 Materials and methods

Chemicals were procured as follows: graphite (power, 99.95% metals basis, 500 mesh; Nanjing Xiaofeng Nanomaterials Co. Ltd); carboxymethyl chitosan (CMC; viscosity average molecular weight 8.6×10^4 Da and DS of 0.9; Shanghai Shifeng Biological Technology Co. Ltd); lactobionic acid (LA; purity > 98%; J&K scientific Co. Ltd); doxorubicin (DOX; purity > 98%; J&K Scientific Co. Ltd); fluorescein isothiocyanate (FITC; Sigma-Aldrich); N-hydroxysuccinimide (NHS; analytical grade. Sigma-Aldrich); 1-(3-dimethyl-aminopropyl)-3-ethylcarbodiimide hydrochloride (EDC; analytical grade; J&K Scientific Co. Ltd); acetic anhydride (analytical grade; Sinopharm Chemical Reagent Co. Ltd); and triethylamine (analytical grade; Sinopharm Chemical Reagent Co. Ltd). Phosphate buffered saline (PBS; pH=7.4) and acetate buffers (pH=5.8) were prepared in-house.

SMMC-7721 cells and L929 cells were provided by the Institute of Biochemistry and Cell Biology, Chinese Academy of Sciences. Dimethyl sulfoxide (DMSO), fetal bovine serum (FBS), phosphate buffered saline (PBS), RPMI 1640 and DMEM media, were supplied by the Shanghai Pumai Biotechnology Co. Ltd. Dialysis membranes (molecular weight cut-offs, 8,000 – 14,000 or 100,000 Da) were also sourced from the Shanghai Pumai Biotechnology Co. Ltd.

2.2 Synthesis and purification of GO-CMC

Graphene oxide was synthesized by using an improved Hummers' method (Hummers & Offeman, 1958). GO-CMC (graphene oxide-carboxymethyl chitosan) was subsequently prepared by first dispersing GO (100 mg) in 25 ml distilled water, then adding NHS (45 mg) and EDC (35 mg) to activate the GO and stirring for 3 h at room temperature. A solution of CMC (200 mg in 20 ml distilled water) was subsequently gradually added to the GO dispersion and the resultant mixture stirred for a further 24 h at room temperature. The reaction product was purified to remove residual GO, CMC and byproducts through dialysis (molecular weight cut-off: 100,000 Da). Dialysis was performed in PBS (2 L) for 1 day then in distilled water (2 L) for 3 days, with the dialysis medium being changed three times per day. GO-CMC was finally obtained from lyophilization of the dialyzed material.

2.3 Synthesis and purification of GO-CMC-FI-LA-Ac

The modification of GO-CMC with FITC and LA to form GO-CMC-FI-LA was undertaken by sequential conjugation. 1 mg FITC was added to an aqueous solution of GO-CMC (25 ml; 2 mg/ml) and stirred for 2 h to obtain GO-CMC-FI. Separately, LA (10 mg) was dissolved in 10 ml of PBS with 25 mg EDC and 20 mg NHS added. This solution was stirred for 3 h at room temperature.

Next, the LA solution was added drop-wise to the GO-CMC-FI solution, and the mixture stirred at room temperature for 24 h to yield GO-CMC-FI-LA. To eliminate any residual amino groups in CMC, 280 μl triethylamine and 160 μl acetic anhydride were added to the mixture and reaction continued for an additional 24 h. The

GO-CMC-FI-LA-Ac product was collected following dialysis (molecular weight cut-off: 8,000 – 14,000 Da) and lyophilization as described in Section 2.2 above.

2.4 Synthesis and purification of GO-CMC-FI-Ac

GO-CMC (50 mg) was dispersed in 25 ml distilled water, and 1 mg FITC added. The resultant solution was allowed to stir for 2h, followed by acetylation for 24h as described in Section 2.3. GO-CMC-FI-Ac was obtained after dialysis (molecular weight cut-off: 8,000 – 14,000 Da) and lyophilization following the same procedures as those described previously.

^{1}H-NMR spectra were obtained using a Bruker DRX 400 nuclear magnetic resonancespectrometer.

2.5 Characterization

^{1}H-NMR spectra were obtained using a Bruker DRX 400 nuclear magnetic resonance spectrometer. Samples of GO, GO-CMC, LA, GO-CMC-FI-Ac, GO-CMC-FI-LA-Ac were dispersed in D_2O before spectra acquisition. Fourier transform infrared (FTIR) spectroscopy was carried out on a Nicolet-Nexus 670 spectrometer (Nicolet Instrument Corporation) over the range 4000-500 cm^{-1} and with a resolution of 2 cm^{-1}. Morphological examination of GO and the modified GO samples was performed using a JEOL 2010F transmission electron microscope (TEM) operated at 200 kV. Thermogravimetric analysis (TGA) was performed using a TG 209F1 (Netzsch Instruments) analyzer, with a heating rate of 20 °C/min and a temperature range of 30-900 °C. Measurements were undertaken in air. Zeta potentials were measured on a Zetasizer Nano ZS system (Malvern). UV-visible (UV-Vis) absorption spectra were recorded on a UV-1800 UV-vis spectrophotometer (Shanghai JingHua Instruments). Confocal laser scanning microscopy was conducted on a Zeiss LSM 510 microscope equipped with an Argon/2 laser, and operated in multichannel model.

2.6 DOX loading

DOX hydrochloride (1-7 mg) and modified GO (5 mg) were dispersed in a pH 9 aqueous solution (5 ml) and stirred for 24 h at room temperature. The products (denoted GO-CMC-FI-LA-Ac-DOX and GO-CMC-FI-Ac-DOX) were collected by ultracentrifugation (12,000 rpm, 30 min) to remove non-conjugated DOX. The drug loading efficiency (LE) and the loading content (LC) (Lu, Wei, Ma, Yang, & Chen, 2012) were calculated by determining the amount of DOX in the centrifugation supernatant. This was quantified through the solution's absorbance at 490 nm, using a UV-vis spectrophotometer (UV-1800, Shanghai JingHua Instruments) (Zhang, et al., 2009). The LE and LC were calculated with reference to a pre-determined DOX concentration curve using the formulae:

$$LC = Md/Mc \times 100\ \%$$

$$LE = Md/Mo \times 100\ \%$$

Where Md is the mass of DOX loaded onto the modified GO, Mc is the mass of modified GO, and Mo is the mass of DOX in the original solution (Hu, et al., 2003; Mohammed, Weston, Coombes, Fitzgerald, & Perrie, 2004).

2.7 DOX release

GO-CMC-FI-LA-Ac-DOX (1 mg) was added to 1 ml of PBS (pH = 7.4) or 1 ml of acetate buffer (pH = 5.8) in a dialysis bag (molecular weight cut-off: 8,000 – 14,000 Da). The bags were then immersed in 25 ml of the same buffer medium. Experiments were performed at 37 ºC in an opaque shaker incubator (HZ-9211K, Taicang Technology). At pre-designed time intervals, aliquots of 1 ml were taken from the release medium and the amount of DOX released was determined by UV-vis spectroscopy. 1 ml of pre-heated buffer solution was added to the release medium to maintain a constant volume. DOX release experiments were performed five times. Analogous experiments were performed under the same conditions with GO-CMC-FI-Ac-DOX (1 mg).

2.8 Cell viability

The MTT assay was used to measure cell viability. In brief, SMMC-7721 cells, a human liver cancer cell line, were seeded into a 96-well plate containing RPMI 1640 medium supplemented with 10 % v/v FBS. The seeding density was 8×10^4 cells/ml, and 200 μl of cell suspension was placed in each well. The plate was loaded into an incubator at 37 ºC under a 5 % CO_2 atmosphere for 24 h. After this time, the medium in each well was removed and replaced with 180 μl of RPMI 1640 supplemented with FBS. 20 μl of a DOX solution in PBS (0.5, 1, 2, 4 μM) or a PBS solution of GO-CMC-FI-LA-Ac-DOX at equivalent DOX concentrations was also added. A negative control was established by adding 20 μl of PBS. Each experiment included six wells for each condition.

After incubation for another 24 h, 20 μl of MTT solution (0.5% w/v) was added followed by incubation for 4 h. Cell viability was determined using the MTT assay; the liquid in each well was removed and replaced with 200 μl DMSO, and the plate shaken for 20 min at 37 ºC. Absorbance was quantified at 570 nm on a microplate reader (Multiskan FC, Thermo Scientific). Control cytotoxicity experiments were performed by testing unloaded GO-CMC-FI-LA-Ac at the same carrier concentrations as described above. Six independent experiments were undertaken.

2.9 Cellular uptake assay

The selective cellular uptake of GO-CMC-FI-LA-Ac-DOX was investigated by confocal microscopy using L929 (mouse fibroblast cells) and SMMC-7721 cells. 2×10^4 cells in 400 μl of DMEM medium or RPMI 1640 medium per well were seeded in each well of 24-well plates and incubated for 24 h. After this time the cells had adhered onto the plate, and the medium was removed. Each well was washed with PBS (400 μl) three times, then 360 μl fresh medium and 40 μl of a solution of GO-CMC-FI-LA-Ac-DOX or GO-CMC-FI-Ac-DOX were added. After incubating for a further 2 h, the cells were fixed with glutaraldehyde (2.5 % v/v in PBS) for 15 min at 4 ºC before being stained with Hoechst 33342 (1 μg/mL) for 15 min at 37 ºC . Finally, the cells were imaged by using a confocal laser-scanning microscope (Carl Zeiss LSM 700) with a 63x oil-immersion objective lens. The confocal experiments were repeated three times.

2.10 *In vitro* selectivity assay

The MTT assay was also used to measure the ability of the formulations to target cancer cells. L929 cells were employed as a non-cancerous control and the lactobionate-free GO-CMC-FI-Ac-DOX compared to GO-CMC-FI-LA-Ac-DOX. L929 cells (180 μl, 8×10^4 cells/ml) or SMMC-7721 cells (180 μl, 8×10^4 cells/ml) were seeded into 96-well plates and incubated for 24 h. 20 μl solutions of GO-CMC-FI-LA-Ac-DOX (40 μM DOX) or GO-CMC-FI-Ac-DOX (40 μM DOX) in the appropriate medium were then added. After incubating for 4 h, the medium was removed and 200 μl fresh medium was added, prior to incubation for an additional 24h. Finally, the MTT assay was conducted to quantify cell viability as described in Section 2.8. Six times independent experiments were performed.

2.11 Statistical analysis

Statistical analysis was carried out using the unpaired Student's t-test on the SAS software (version 9.0). A value of $p < 0.05$ was considered statistically significant. Data are annotated with * for $p < 0.05$, ** for $p < 0.01$, and *** for $p < 0.001$.

3. Results and discussion

3.1 Preparation and characterization of modified GO

The synthetic strategy underlying this work is presented in Fig. 1. GO was first generated using a modified Hummers' method (Hummers & Offeman, 1958) and CMC with available amino groups next used to modify the GO, before the FITC fluorophore was conjugated to the CMC. The targeting ligand LA was attached to the composite via the remaining unreacted amino groups on CMC. Finally, the functionalized GO nanocomposite was acetylated to eliminate any residual free amino groups on CMC (Fig. 1a). Subsequent mixing of this with DOX permits the drug to be adsorbed (Fig. 1b).

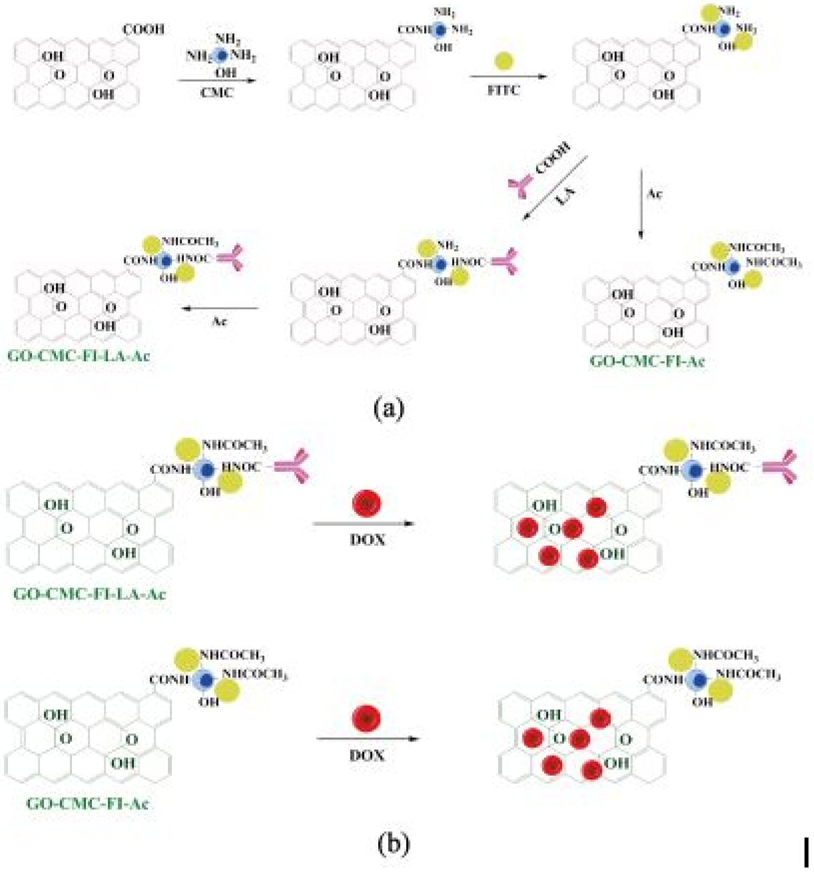

Fig. 1. The synthetic strategy used in this work: (a) the synthesis of functionalized GO materials and (b) DOX loading.

The formation of the GO-CMC-FI-Ac and GO-CMC-FI-LA-Ac conjugates were confirmed via ^{1}H-NMR spectroscopy, as shown in Fig. S1 (Supporting Information). GO does not display any salient proton signals, since all its COOH and OH groups will undergo rapid proton transfer with the D_2O solvent. After reaction with CMC, a resonance at 4.5 ppm is observed, corresponding to the -CH_2-COO- protons at the C_6 position of CMC (Prabaharan, Reis, & Mano, 2007; Sun, et al., 2006), together with a series of peaks in the 3 – 4 ppm region from the CMC rings. Further modification of the CMC with FITC and LA can also clearly be confirmed from the spectra of GO-CMC-FI and GO-CMC-FI-LA. Peaks at 6.4 ppm in the spectrum of these conjugates are attributable to FI, and GO-CMC-FI-LA additionally exhibits resonances at 3.8-4.3 ppm from the LA component (Fu, et al., 2014). The final acetylation of the remaining unreacted amines of CMC led to the formation of

GO-CMC-FI-Ac and GO-CMC-FI-LA-Ac. The $-CH_3$ protons of the acetyl groups appear at 1.87 ppm in proton NMR; both conjugates show this peak, which indicates the success of the acetylation reaction (Cao, et al., 2015).

Fourier transform infrared (FTIR) spectroscopy was also conducted to confirm the synthesis and modification of the GO. Fig. 2 shows the spectra of the materials obtained at each step of the synthesis. The FTIR spectra of GO, CMC and GO-CMC are given in Fig 2a. The presence of the oxygen functionalities on GO was confirmed by the absorbance peaks at 1731 cm^{-1}, 1400 cm^{-1}, 1230 cm^{-1} and 1066 cm^{-1}, which respectively correspond to C=O, O-H (carboxylic acid), C-O (epoxy), and C-O (alkoxy) groups. The broad peak at 3400 cm^{-1} in the spectra of GO corresponds to O-H stretching mode, and that at 1626 cm^{-1} to the bending vibrations of adsorbed water molecules, as has been reported in the literature (Liao, Chen, Quan, Yu, & Zhao, 2012).

The characteristic peaks of the amino group on CMC at 3373 cm^{-1} and 3281 cm^{-1} are less obvious when CMC is linked to GO. The spectrum of GO-CMC shows absorbance bands corresponding to the amide group at 1669 cm^{-1} (C=O) and 1558 cm^{-1} (C-N). This indicates that CMC was successfully grafted to the GO. The FTIR spectra of GO-CMC-FI-Ac and GO-CMC-FI-LA-Ac are depicted in Fig 2b. After further modification of GO-CMC with LA, a new peak at 1706 cm^{-1} corresponding to the amide C=O stretching vibration was observed. Peaks at 1420 cm^{-1} for GO-CMC-FI-Ac and 1405 cm^{-1} for GO-CMC-FI-LA-Ac are assigned to the acetyl methyl group. FITC was present only in very small amounts, and thus its characteristic peaks are swamped by vibrations from the other components of the system and are not visible in the IR spectra.

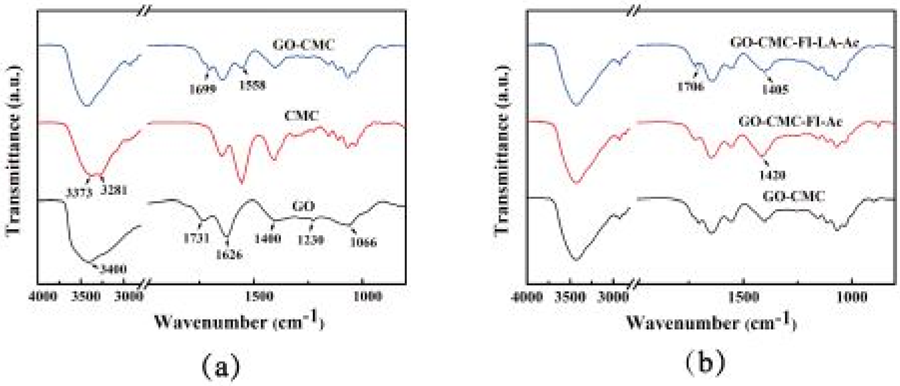

Fig. 2. FTIR spectra of (a) GO, CMC, and GO-CMC; and, (b) GO-CMC, GO-CMC-FI-Ac, and GO-CMC-FI-LA-Ac.

Further, Zeta potential measurements were carried out to verify the surface modification of GO (Table 1). The zeta potential of pure GO was negative (-38.3 ± 0.7 mV) due to the presence of a large number of carboxyl and hydroxyl groups on its surface. When GO was modified with CMC, amino groups replaced some of the carboxyl groups and the zeta potential became less negative accordingly (GO-CMC: -32.6 ± 0.21 mV). Further conjugation with FITC and LA, followed by acetylation added a number of acidic groups to the system, and hence the potential decreased (to -40.1 ± 1.2 mV for GO-CMC-FI-LA-Ac). The zeta potential of GO-CMC-FI-Ac is somewhat less negative than that of GO-CMC-FI-LA-Ac, which is consistent with the presence of additional COOH groups from LA in the latter.

Table 1. Zeta potential values. Measurements were recorded three times and are reported as mean ± S.D.

	GO	**GO-CMC**	**GO-CMC-FI-LA-Ac**	**GO-CMC-FI-Ac**
Zeta potential (mV)	-38.3 ± 0.7	-32.6 ± 0.21	-40.1 ± 1.2	-36.4 ± 0.6

To quantify the compositions of the conjugates, thermogravimetric analysis was performed. The literature reports that when TGA is performed on the raw materials, at 900 °C CMC, FI, LA and Ac all exhibit 100% weight loss (Lv, et al., 2016; Wang, et al., 2013; Cao, et al., 2015; Wen, et al., 2013). The data obtained in this work are given in Fig. 3. At 900 °C, GO, GO-CMC, GO-CMC-FI-Ac and GO-CMC-FI-LA-Ac have remnant masses of 26%, 15%, 14% and 10%, respectively. Therefore, by comparison of these values, it can be estimated that the weight contents of the grafted CMC and FI-Ac in GO-CMC-FI-Ac are 39% and 7%. In GO-CMC-FI-LA-Ac, the weight contents of the grafted CMC, and FI-LA-Ac are 28% and 34%, respectively. Full details of the calculations performed are given in the Supporting Information, Table S1.

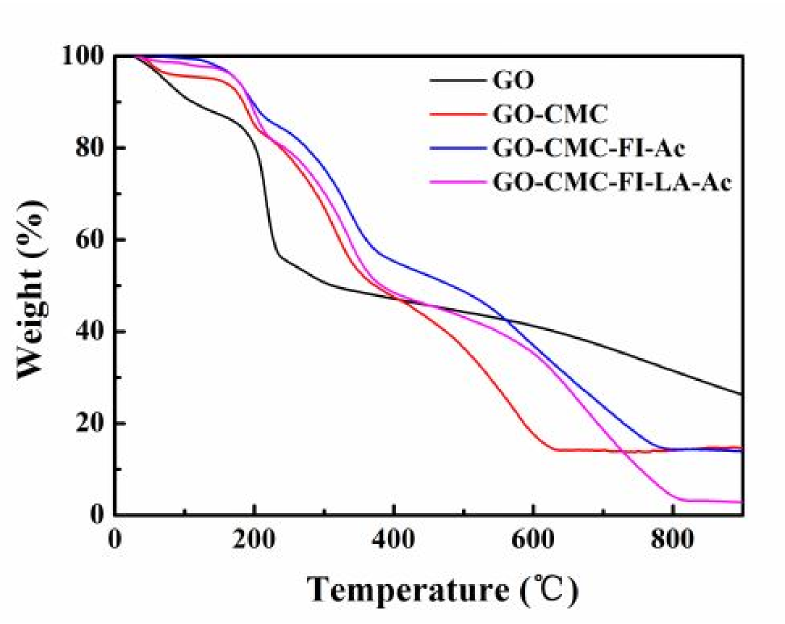

Fig. 3. TGA curves of GO, GO-CMC, GO-CMC-FI-Ac and GO-CMC-FI-LA-Ac.

The morphology of the modified GO materials was investigated by transmission electron microscopy (TEM), and the results are given in Fig. 4. The intrinsic lamellar structure of GO is clearly visible in Fig. 4a. The images of GO-CMC-FI-LA-Ac (Fig. 4b) and GO-CMC-FI-Ac (Fig. 4c) show the materials to be smooth and uniform, with the initial layered structure of GO remaining intact. The materials depicted in Fig. 4b and 4c have some darker patches on the sheet: these are a result of the functionalization process, as has previously been reported (Yang, et al., 2016).

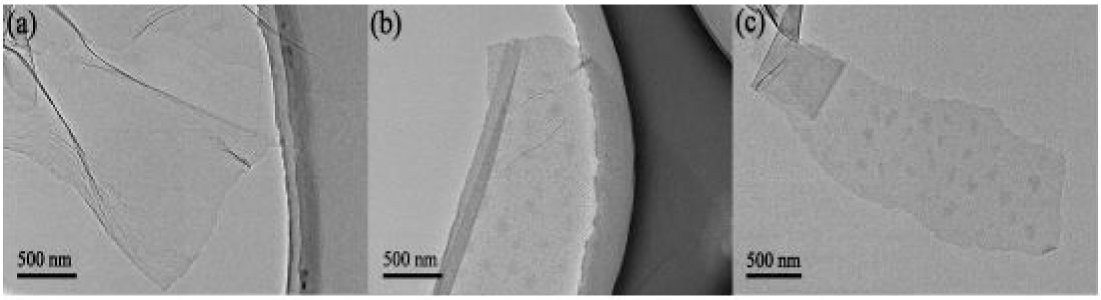

Fig. 4. TEM images of (a) GO, (b) GO-CMC-FI-LA-Ac, and (c) GO-CMC-FI-Ac.

3.2 DOX loading and release

Previously, it has been shown that DOX can be adhered onto the surface of GO via strong π-π stacking interactions (Zheng, et al., 2011). The drug loading efficiency (LE) and the drug loading content (LC) were first determined to evaluate the drug loading performance (Fig. 5a). At pH 9, the LC of GO-CMC-FI-LA-Ac-DOX was 98 % when the initial DOX concentration was 1 mg/ml or less, but decreased to 88 % when the DOX concentration in the starting solution was increased to 1.4 mg/ml. The LE of GO-CMC-FI-LA-Ac-DOX increased with the drug concentration up to 1 mg/ml, reaching a maximum of 96 %; if the concentration was further increased beyond this point, the LE decreased. The DOX loading performance of GO-CMC-FI-Ac-DOX is similar. Thus, a DOX : modified GO ratio of 1:1 was deemed best for preparing GO-CMC-FI-LA-Ac-DOX and GO-CMC-FI-Ac-DOX.

The release of DOX from the modified GO samples was next studied (Fig. 5b). In PBS buffer at pH 7.4, corresponding to the normal physiological pH, the drug is released in a slow and sustained manner (reaching ~20 % after 72 h). In slightly acidic solutions (pH 5.8) equivalent to the reduced pH microenvironment typical of cancerous cells (Gerweck & Seetharaman, 1996), the release rate is significantly enhanced. The amount of DOX released after 72 h is approximately 45 %. GO-CMC-FI-Ac-DOX and GO-CMC-FI-LA-Ac-DOX behave very similarly at both pHs. The greater amount of release seen at pH 5.8 is caused by the π-π stacking interactions between DOX and GO being weaker at this lower pH. These results indicate that GO-CMC-FI-LA-Ac or GO-CMC-FI-Ac are potentially useful carriers which can selectively release their drug cargo in tumors, and avoid deleterious side effects in normal tissue.

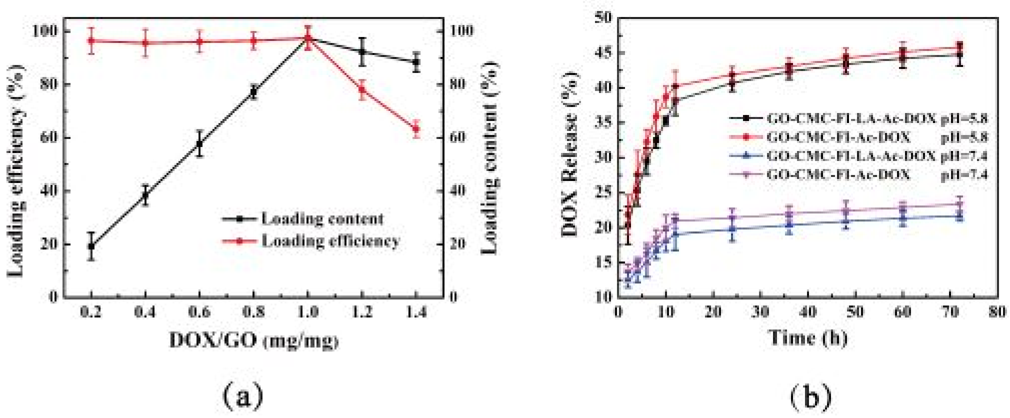

Fig. 5. (a) The drug loading performance of GO-CMC-FI-LA-Ac at pH 9. Data are reported as mean ± S.D. from three independent experiments.

(b) The release of DOX at pH 7.4 and pH 5.8. Data are reported as mean ± S.D. from five independent experiments.

3.3 Therapeutic efficacy and biocompatibility

The cytotoxicity of GO-CMC-FI-LA-Ac-DOX towards SMMC-7721 cells was explored after a 24 h incubation time. The data obtained are given in Fig. 6a. When SMMC-7721 cells were treated with free DOX, they generally showed lower viability than after treatment with GO-CMC-FI-LA-Ac-DOX or GO-CMC-FI-LA-DOX containing equivalent amounts of the drug. This is a relatively small effect, however, and the GO-CMC-FI-LA-Ac-DOX material in particular shows cytotoxicity values close to those of the free drug. The dose-response behavior is also more marked with the GO conjugates: at an equivalent concentration of 4 μM DOX, GO-CMC-FI-LA-Ac-DOX is more effective than the free drug, while GO-CMC-FI-Ac-DOX is equally efficacious.

The biocompatibility of the modified GO materials was determined by evaluating the cytotoxicity of the drug-free systems (Fig. 6b). Experiments were performed with the amounts of materials required to carry DOX concentrations of 0-4 μM. Both GO-CMC-FI-LA-Ac and GO-CMC-FI-Ac have generally high biocompatibility, with GO-CMC-FI-LA-Ac showing cell viability of > 80 % even at a concentration of 2.4 mg/L. GO-CMC-FI-Ac is slightly more toxic, but even here the viability is generally high. Hence, it is clear that the modified GO materials have good biocompatibility and the therapeutic efficacy of the drug-loaded GO-CMC-FI-LA-Ac-DOX and GO-CMC-FI-Ac-DOX materials is similar to that of pure DOX.

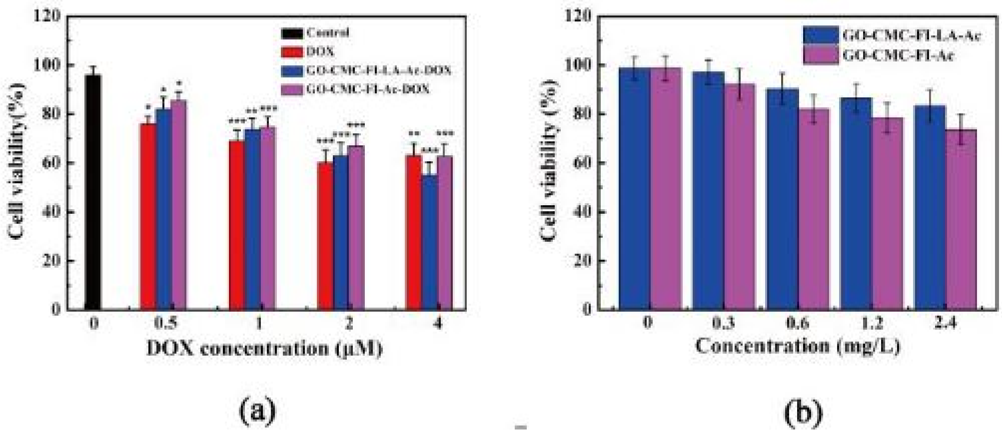

Fig. 6. The results of MTT viability assays of SMMC-7721 cells treated with (a) free DOX, GO-CMC-FI-LA-Ac-DOX and GO-CMC-FI-Ac-DOX at DOX concentrations of 0 – 4 μM for 24 h; (b) drug-free GO-CMC-FI-LA-Ac and GO-CMC-FI-Ac. Data are reported as mean ± S.D. from six independent experiments. Asterisks indicate statistical significance, with * denoting $p < 0.05$, ** $p < 0.01$, and *** $p < 0.001$ with respect to the control group.

To determine the selectivity of the LA-targeted drug delivery system, L929 and SMMC-7721 cells were treated with GO-CMC-FI-LA-Ac-DOX and GO-CMC-FI-Ac-DOX. Cellular uptake of the DOX-loaded materials by SMMC-7721 cells (cancerous cells, which express ASGPR receptors) and L929 cells (which do not express ASGPR) (Li, et al., 2014), were probed by confocal microscopy; the results are depicted in Fig. 7. The pure cells are stained blue, and the green fluorescence of FITC and red fluorescence of DOX can be used to track the presence of the drug and modified GO samples. The images clearly show higher uptake of GO-CMC-FI-LA-Ac-DOX than GO-CMC-FI-Ac-DOX by SMMC-7721 cells. This is because of the ability of the LA moiety in the former to bind with the surface ASGPR receptors on the cells. In contrast, none of the systems is taken up to any observable extent by L929 cells, thus proving the importance of LA-ASGPR interactions in promoting uptake of the GO materials.

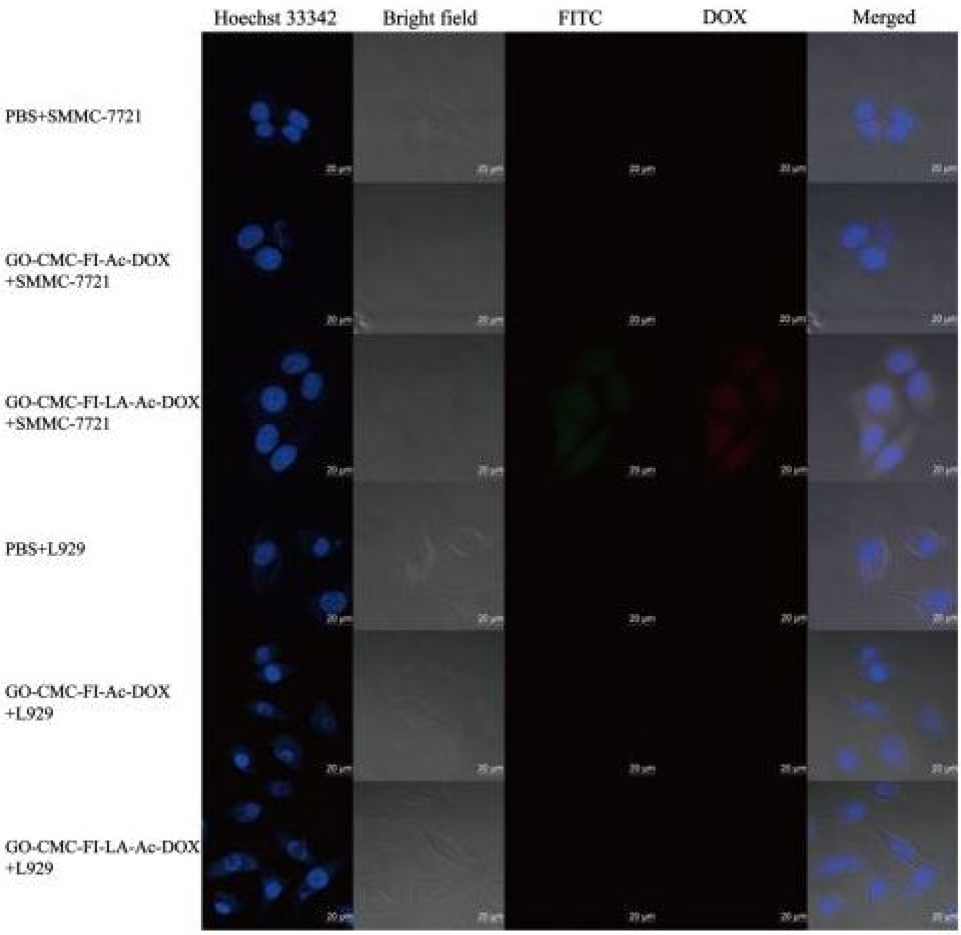

Fig. 7. Confocal microscopy images of SMMC-7721 and L929 cells treated with GO-CMC-FI-LA-Ac-DOX or GO-CMC-FI-Ac-DOX (DOX concentration: 4 μM) for

2h. Red fluorescence arises from DOX, and green fluorescence from FITC.

Further, the targeted ability of GO-CMC-FI-LA-Ac-DOX to target specific cells was also explored (Fig. 8). In these experiments, the cells were exposed to the DOX-loaded GOs for 2 h, before the medium was removed and the cells were allowed to incubate for a further 24 h. It is clear that the SMMC-7721 cells have lower viability (~ 50 %) after treatment with GO-CMC-FI-LA-Ac-DOX than L929 cells do after the same treatment (~ 92 %). However, both SMMC-7721 and L929 cells treated with GO-CMC-FI-Ac-DOX have high viability (~ 90 %). Therefore, the LA functionality of the GO-CMC-FI-LA-Ac-DOX enables the drug cargo to be selectively delivered to liver cancer cells. This suggests that these novel drug carriers may be highly potent chemotherapeutic drug carriers able to mitigate against the unpleasant side effects which usually arise owing to the non-selectivity of such treatments.

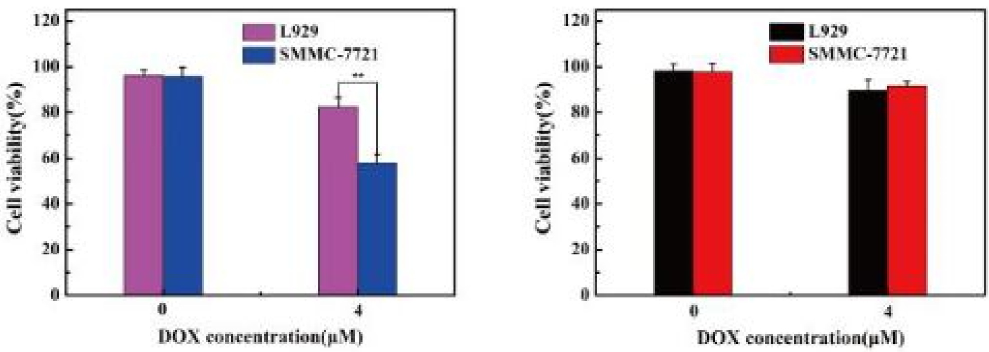

(a) (b)

Fig. 8. The viability of SMMC-7721 and L929 cells after treatment with (a) GO-CMC-FI-LA-Ac-DOX, and (b) GO-CMC-FI-Ac-DOX for 2 h, followed by replacement of the medium with DOX-free fresh medium and incubating the cells for an additional 24 h. Data are reported as mean ± S.D. from six independent experiments. * denotes $p < 0.05$, ** $p < 0.01$, and *** $p < 0.001$ when comparing theSMMC-7721 experiments to the L929 data.

Conclusions

A novel anticancer drug delivery system based on multifunctionalized graphene oxide (GO) has been developed to provide targeted delivery to liver cancers. The system is prepared by sequential functionalization of GO with carboxymethyl chitosan, fluorescein isothiocyanate, and lactobionic acid (LA), followed by acylation to avoid the presence of free amino groups. A control system was prepared without lactobionic acid conjugation. The model anticancer drug doxorubicin (DOX) was subsequently loaded onto the system by physisorption. The resultant formulation has high drug loading content and efficiency (> 96 %) and pH-sensitive release. Release is both more rapid and reaches a greater extent at the mildly acidic pH typical of the tumor microenvironment than at pH 7.4. *In vitro* tests on a liver cancer cell line demonstrated that while the GO composites are not cytotoxic, the DOX-loaded systems are effective in inducing cell death, being almost as potent as the free drug. Further, the DOX-loaded lactobionic acid conjugated GO system was able to selectively induce the death of cancerous cells, but was non-toxic to a non-cancerous cell line. This is thought to occur due to the selective recognition of LA by the asialoglycoprotein receptors which are over-expressed on cancerous hepatic cells. These promising results show that the GO-based systems generated in this work have great potential for targeted anticancer therapy *in vivo*.

Acknowledgements

This investigation was supported by the Biomedical Textile Materials “111 Project” of the Ministry of Education of China (No. B07024), and the UK-China Joint Laboratory for Therapeutic Textiles.

References

Agnihotri, S. A., Mallikarjuna, N. N., & Aminabhavi, T. M. (2004). Recent advances on chitosan-based micro-and nanoparticles in drug delivery. *Journal of controlled release, 100*(1), 5-28.

Allen, T. M., & Cullis, P. R. (2013). Liposomal drug delivery systems: from concept to clinical applications. *Advanced drug delivery reviews, 65*(1), 36-48..

Arora, S., Ali, J., Ahuja, A., Khar, R. K., & Baboota, S. (2005). Floating drug delivery systems: a review. *AAPS PharmSciTech, 6*(3), E372-E390.

Ashwell, G., & Harford, J. (1982). Carbohydrate-specific receptors of the liver. *Annual review of biochemistry, 51*(1), 531-554.

Bae, Y. H., & Park, K. (2011). Targeted drug delivery to tumors: myths, reality and possibility. *Journal of Controlled Release, 153*(3), 198.

Bamrungsap, S., Zhao, Z., Chen, T., Wang, L., Li, C., Fu, T., & Tan, W. (2012). Nanotechnology in therapeutics: a focus on nanoparticles as a drug delivery system. *Nanomedicine, 7*(8), 1253-1271.

Bao, H., Pan, Y., Ping, Y., Sahoo, N. G., Wu, T., Li, L., Li, J., & Gan, L. H. (2011). Chitosan-Functionalized Graphene Oxide as a Nanocarrier for Drug and Gene Delivery. *Small, 7*(11), 1569-1578.

Bianco, A., Kostarelos, K., & Prato, M. (2005). Applications of carbon nanotubes in drug delivery. *Current opinion in chemical biology, 9*(6), 674-679.

Bruschi, M. L. (2015). Development of Drug Delivery Systems and Quality by Design. *Recent patents on drug delivery & formulation*.

Cao, X., Tao, L., Wen, S., Hou, W., & Shi, X. (2015). Hyaluronic acid-modified multiwalled carbon nanotubes for targeted delivery of doxorubicin into cancer cells. *Carbohydrate Research,* 405, 70-77.

Cao, Y., He, Y., Liu, H., Luo, Y., Shen, M., Xia, J., & Shi, X. (2015). Targeted CT imaging of human hepatocellular carcinoma using low-generation dendrimer-entrapped gold nanoparticles modified with lactobionic acid. *Journal of Materials Chemistry B, 3*(2), 286-295.

Chen, G., Li, D., Li, J., Cao, X., Wang, J., Shi, X., & Guo, R. (2015). Targeted doxorubicin delivery to hepatocarcinoma cells by lactobionic acid-modified laponite nanodisks. *New Journal of Chemistry, 39*(4), 2847-2855.

Debbage, P. (2009). Targeted drugs and nanomedicine: present and future. *Current pharmaceutical design, 15*(2), 153-172.

Faria, P. C. B. D., Santos, L. I. D., Coelho, J. P., Ribeiro, H. B., Pimenta, M. A., Ladeira, L. O., Gomes, D. A., Furtado, C. A., & Gazzinelli, R. T. (2014). Oxidized Multiwalled Carbon Nanotubes as Antigen Delivery System to Promote Superior CD8+T Cell Response and Protection against Cancer. *Nano letters, 14*(9), 5458-5470.

Feazell, R. P., Nakayama-Ratchford, N., Dai, H., & Lippard, S. J. (2007). Soluble single-walled carbon nanotubes as longboat delivery systems for platinum (IV) anticancer drug design. *Journal of the American Chemical Society, 129*(27), 8438-8439.

Fu, F., Wu, Y., Zhu, J., Wen, S., Shen, M., & Shi, X. (2014). Multifunctional lactobionic acid-modified dendrimers for targeted drug delivery to liver cancer cells: investigating the role played by PEG spacer. *ACS Applied Materials & Interfaces, 6*(18), 16416-16425.

Gerweck, L. E., & Seetharaman, K. (1996). Cellular pH gradient in tumor versus normal tissue: potential exploitation for the treatment of cancer. *Cancer research, 56*(6), 1194-1198.

Gong, J., Chen, M., Zheng, Y., Wang, S., & Wang, Y. (2012). Polymeric micelles drug delivery system in oncology. *Journal of Controlled Release, 159*(3), 312-323.

Hummers Jr, W. S., & Offeman, R. E. (1958). Preparation of graphitic oxide. *Journal of the American Chemical Society, 80*(6), 1339-1339.

Hu, Y., Jiang, X., Ding, Y., Zhang, L., Yang, C., Zhang, J., Chen, J., & Yang, Y. (2003). Preparation and drug release behaviors of nimodipine-loaded poly (caprolactone)–poly (ethylene oxide)–polylactide amphiphilic copolymer nanoparticles. *Biomaterials, 24*(13), 2395-2404.

Jayakumar, R., Prabaharan, M., Kumar, P. S., Nair, S. V., & Tamura, H. (2011). Biomaterials based on chitin and chitosan in wound dressing applications. *Biotechnology Advances, 29*(3), 322-337.

Liao, G., Chen, S., Quan, X., Yu, H., & Zhao, H. (2012). Graphene oxide modified

gC_3N_4 hybrid with enhanced photocatalytic capability under visible light irradiation. *Journal of Materials Chemistry, 22*(6), 2721-2726.

Li, H., Cui, Y., Liu, J., Bian, S., Liang, J., Fan, Y., & Zhang, X. (2014). Reduction breakable cholesteryl pullulan nanoparticles for targeted hepatocellular carcinoma chemotherapy. *Journal of Materials Chemistry B, 2*(22), 3500-3510.

Liu, Z., Chen, K., Davis, C., Sherlock, S., Cao, Q., Chen, X., & Dai, H. (2008). Drug delivery with carbon nanotubes for in vivo cancer treatment. *Cancer Research, 68*(16), 6652-6660.

Liu, Z., Robinson, J. T., Sun, X., & Dai, H. (2008). PEGylated nanographene oxide for delivery of water-insoluble cancer drugs. *Journal of the American Chemical Society, 130*(33), 10876-10877.

Long, Y., Wang, J., Tao, C. A., Zhu, H., Lv, Y., & Li, N. (2013). The loading and release properties of a novel drug carrier for benazepril based on nano graphene oxide. *Journal of Controlled Release, 1*(172), e88-e89.

Luo, Y., Teng, Z., & Wang, Q. (2012). Development of zein nanoparticles coated with carboxymethyl chitosan for encapsulation and controlled release of vitamin D3. *Journal of Agricultural and Food Chemistry, 60*(3), 836-843.

Lu, Y. J., Wei, K. C., Ma, C. C. M., Yang, S. Y., & Chen, J. P. (2012). Dual targeted delivery of doxorubicin to cancer cells using folate-conjugated magnetic multi-walled carbon nanotubes. *Colloids and Surfaces B: Biointerfaces, 89*, 1-9.

Lv, M., Zhang, Y., Liang, L., Wei, M., Hu, W., Li, X., & Huang, Q. (2012). Effect of graphene oxide on undifferentiated and retinoic acid-differentiated SH-SY5Y cells line. *Nanoscale, 4*(13), 3861-3866.

Lv, Y., Tao, L., Bligh, S. A., Yang, H., Pan, Q., & Zhu, L. (2016). Targeted delivery and controlled release of doxorubicin into cancer cells using a multifunctional graphene oxide. *Materials Science and Engineering: C*, 59, 652-660.

Ma, X., Tao, H., Yang, K., Feng, L., Cheng, L., Shi, X., Li, Y., Guo, L., & Liu, Z. (2012). A functionalized graphene oxide-iron oxide nanocomposite for magnetically targeted drug delivery, photothermal therapy, and magnetic resonance imaging. *Nano Research, 5*(3), 199-212.

Meng, L., Zhang, X., Lu, Q., Fei, Z., & Dyson, P. J. (2012). Single walled carbon nanotubes as drug delivery vehicles: targeting doxorubicin to tumors. *Biomaterials, 33*(6), 1689-1698.

Mohammed, A. R., Weston, N., Coombes, A. G. A., Fitzgerald, M., & Perrie, Y. (2004). Liposome formulation of poorly water soluble drugs: optimisation of drug loading and ESEM analysis of stability. *International journal of pharmaceutics, 285*(1), 23-34.

Prabaharan, M., Reis, R. L., & Mano, J. F. (2007). Carboxymethyl chitosan-graft-phosphatidylethanolamine: Amphiphilic matrices for controlled drug delivery. *Reactive and Functional Polymers, 67*(1), 43-52.

Roosen, J., Spooren, J., & Binnemans, K. (2014). Adsorption performance of functionalized chitosan-silica hybrid materials toward rare earths. *Journal of Materials Chemistry A, 2*(45), 19415-19426.

Shan, C., Yang, H., Han, D., Zhang, Q., Ivaska, A., & Niu, L. (2010). Graphene/AuNPs/chitosan nanocomposites film for glucose biosensing. *Biosensors and Bioelectronics, 25*(5), 1070-1074

Song, X., Luo, X., Zhang, Q., Zhu, A., Ji, L., & Yan, C. (2015). Preparation and characterization of biofunctionalized chitosan/Fe_3O_4 magnetic nanoparticles for application in liver magnetic resonance imaging. *Journal of Magnetism and Magnetic Materials, 388*, 116-122.

Sun, L., Du, Y., Fan, L., Chen, X., & Yang, J. (2006). Preparation, characterization and antimicrobial activity of quaternized carboxymethyl chitosan and application as pulp-cap. *Polymer, 47*(6), 1796-1804.

Sun, X., Liu, Z., Welsher, K., Robinson, J. T., Goodwin, A., Zaric, S., & Dai, H. (2008). Nano-graphene oxide for cellular imaging and drug delivery. *Nano Research, 1*(3), 203-212.

Tao, C. A., Wang, J., Qin, S., Lv, Y., Long, Y., Zhu, H., & Jiang, Z. (2012). Fabrication of pH-sensitive graphene oxide-drug supramolecular hydrogels as controlled release systems. *Journal of Materials Chemistry, 22*(47), 24856-24861.

Vaghani, S. S., Patel, M. M., & Satish, C. S. (2012). Synthesis and characterization of pH-sensitive hydrogel composed of carboxymethyl chitosan for colon targeted delivery of ornidazole. *Carbohydrate Research, 347*(1), 76-82.

Wang, J., Chen, B., Zhao, D., Peng, Y., Zhuo, R. X., & Cheng, S. X. (2013). Peptide decorated calcium phosphate/carboxymethyl chitosan hybrid nanoparticles with improved drug delivery efficiency. *International Journal of Pharmaceutics, 446*(1), 205-210.

Wen, H., Dong, C., Dong, H., Shen, A., Xia, W., Cai, X., & Shi, D. (2012). Engineered Redox - Responsive PEG Detachment Mechanism in PEGylated Nano-Graphene Oxide for Intracellular Drug Delivery. *Small, 8*(5), 760-769.

Wen, S., Liu, H., Cai, H., Shen, M., & Shi, X. (2013). Targeted and pH-responsive delivery of doxorubicin to cancer cells using multifunctional dendrimer-modified multi-walled carbon nanotubes. *Advanced Healthcare Materials, 2*(9), 1267-1276.

Yang, H., Bremner, D. H., Tao, L., Li, H., Hu, J., & Zhu, L. (2016). Carboxymethyl chitosan-mediated synthesis of hyaluronic acid-targeted graphene oxide for cancer drug delivery. *Carbohydrate Polymers, 135*, 72-78.

Zhang, D., Zhang, Z., Liu, Y., Chu, M., Yang, C., Li, W., Shao, Y., Yue, Y., & Xu, R. (2015). The short-and long-term effects of orally administered high-dose reduced graphene oxide nanosheets on mouse behaviors. *Biomaterials, 68*, 100-113.

Zhang, L., Xia, J., Zhao, Q., Liu, L., & Zhang, Z. (2010). Functional graphene oxide as a nanocarrier for controlled loading and targeted delivery of mixed anticancer drugs. *Small, 6*(4), 537-544.

Zhang, W., Zhang, Z., & Zhang, Y. (2011). The application of carbon nanotubes in target drug delivery systems for cancer therapies. *Nanoscale Research Letters, 6*(1), 1-22.

Zhang, X., Meng, L., Lu, Q., Fei, Z., & Dyson, P. J. (2009). Targeted delivery and controlled release of doxorubicin to cancer cells using modified single wall carbon nanotubes. *Biomaterials, 30*(30), 6041-6047.

Zheng, H., Zhang, X., Yin, Y., Xiong, F., Gong, X., Zhu, Z., Lu, B., & Xu, P. (2011). In vitro characterization, and in vivo studies of crosslinked lactosaminated carboxymethyl chitosan nanoparticles. *Carbohydrate Polymers, 84*(3), 1048-1053.

Zhu, X., Xie, Y., Zhang, Y., Huang, H., Huang, S., Hou, L.,Zhang, H., Li, Z., Shi, J., & Zhang, Z. (2014). Thermo-sensitive liposomes loaded with doxorubicin and lysine modified single-walled carbon nanotubes as tumor-targeting drug delivery system. *Journal of Biomaterials Applications*, *29*(5), 769-779.